Al-Qadisiyah JournalFor Engineering Sciences 19 (2026) 098 – 109

Contents lists available at: http://qu.edu.iq

Al-Qadisiyah Journal for Engineering Sciences

Journal homepage: https://qjes.qu.edu.iq

Research Paper

Thermodynamic analysis of small-scale CSP based on ORC systems compared with PV systems in North Africa zone. (Algeria as a case study)

A. Touil[1,2]✉, ***D. Nehari***[3,4], ***M. Laissaoui***[5], ***and H. Benzaama***[6]

[1]*Ecole Nationale Polytechnique d'Oran, Algeria.*
[2]*Scientific and Technical Research Center on Arid Regions CRSTRA, Biskra, Algeria.*
[3]*University Center of Ain Témouchant, Algeria.*
[4]*Laboratory of Applied Hydrology and Environment, University of Ain Temouchent, Algeria.*
[5]*Centre de Developpement des Energies Renouvelables BP. 62 Route de l'Observatoire Bouzareah 16340 Alger, Algeria.*
[6]*National Polytechnic School of Oran, Algeria.*

ARTICLE INFO

Article history:
Received 22 January 2025
Received in revised form 03 October 2025
Accepted 10 December 2025

keyword:
Thermodynamic analysis
Concentrating solar power
Organic Rankine Cycle each
Photovoltaic
North Africa
Algeria

ABSTRACT

This study presents a simulation of electricity generation systems utilizing solar energy, employing TRNSYS and EES software to address the energy needs of isolated areas in Algeria. Two solar energy systems were compared: the CSP-ORC and the Photovoltaic, analyzed across three regions: Adrar, Illizi, and El-Bayadh. The CSP-ORC system was enhanced by incorporating components for optimizing the operation of the pump within the ORC, as well as integrating a solar photovoltaic system with battery storage at a capacity of 50 kW. The estimated electrical power generated by the studied systems is approximately 1 MW. We compared the technical performance of a 1 MW s-ORC system with thermal energy storage against that of a solar photovoltaic system of the same capacity. This analysis underscores the viability of both CSP-ORC and PV systems for electricity generation in isolated arid regions of Algeria. However, the superior performance of the PV system, particularly during the winter months, suggests that while CSP-ORC systems are promising, they may require further enhancements or integrated solutions (such as hybrid systems) to improve output and reliability across all seasons. The economic analysis highlights the cost-effectiveness of PV systems, which have lower investment, maintenance costs, and LCOE than CSP-ORC. The lowest LCOE (0.0311 €/kWh) and fastest payback (3.62 years) were observed in Illizi for PV, while CSP-ORC had the highest LCOE in El-Bayadh. Environmentally, PV reduces 55.2 tons of CO_2 emissions in Illizi, whereas CSP-ORC, generating more electricity, prevents 84 tons. Both systems significantly cut emissions compared to diesel generators.

1. Introduction

According to IRENA's 2018 annual report, "Global Energy Transformation - Roadmap to 2050", the renewable energy mix is expected to shift significantly, with solar and wind accounting for more than half of total renewable energy generation [1], The share of renewable energy in the energy sector is expected to increase to 85% in 2050. While renewable energy currently represents less than 60% of total energy consumption, direct use of renewable energy will account for a large proportion of energy use in industry, buildings and transportation. Approximately a quarter of this will come from solar thermal energy and the rest will come from geothermal and other renewable sources [2]. Extensive research has been carried out in the field of solar thermal co-generation using the Organic Rankine Cycle (ORC) systems. ORC systems are one of the most common and competitive technologies for efficiently converting solar energy into generated energy, especially small scall power and isolated areas. Pantelis N. Botsariset al [3], developed a simulation model of the current power plant, which uses a solar thermal field with parabolic trough collectors in addition to the Organic Rankine Cycle, The model, designed using the TRNSYS v.17 software package, was validated against real operating conditions, a power plant located near the village of Zilot in Xanthi, in northeastern Greece, the simulated power plant operates on a 234 kW solar parabolic trough collectors and a 5 kW ORC engine.The model is reliable because of small deviations. Their work aims to promote the growth of solar thermal energy in Greece, through the development of a software-based model of the PTC power plant along with ORC. Related to solar applications, He et al. [4] Developed a simulation model of an integrated thermal solar power generation system with ORC plant and analyzed the system performance taking into account four typical days. [4] investigated the performance of a 250 kW control circuit coupled to compound parabolic sensors under design-deformed conditions due to fluctuations in ambient temperature and heat transfer fluid (HTF) mass flow rate. Borunda et al. [5] presented a study on a small CSP plant coupled to an ORC engine, including a new configuration using directly useful energy to power the ORC engine and load the TES. Tocci et al. [6] provided an overview of the state of the art in ORC technology for low power applications. The authors concluded that ORC systems for the production of powers between 1 and 100 kW still have low absorption in the market. Choi Yun Chai andhyung-chuljung [7] presented a study ,on a small CSP plant, a 1kWe solar ORC with a parabolic trough collector (PTC), used in isolate village in MALAYZIA.

*Corresponding Author.
E-mail address: aektouil@yahoo.fr ; Tel: (+21) 355-070 4178 (A. Touil)

https://doi.org/10.30772/qjes.2025.156874.1486

Nomenclature

A_{SF}	Solar field colleting area (m^2)	C_{fluid}	Specific heat capacity of the fluid $J/(kgC°)$.
A_{EL}	Annual electricity production (MWh/year)	T_{fluid}	The temperature of the fluid ($C°$).
P_{EL}	ORC net electrical power (MW)	$A_{exposed}$	The exposed surface area for heat losses.
T_{amb}	Ambient temperature (C°)	U_{losses}	The heat transfer coefficient.
$A_{optique}$	The optical aperture area of the solar field (m^2)	V	The voltage (V).
$\eta_{optique}$	The global optical efficiency.	I	Current (A).
$\eta_{thermique}$	The thermal efficiency of the solar field.	P	The power output (W).
η_{ORC}	The thermal-to-mechanical conversion efficiency of the ORC.	C_{pv}	Thermal capacitance of the PV cell ($J/C°$).
T_{source}	The temperature of the thermal fluid exiting the solar receivers ($C°$).	η_{pv}	Electrical efficiency of the PV cell.
T_{cond}	The condensation temperature of the ORC working fluid ($C°$).	A_{pv}	Surface area of the PV panel (m^2).
P_{elec}	The net electrical power output (W)	H	Heat transfer coefficient $W/(m^2C°)$.
$E_{solaire}$	The total solar energy incident on the system (W).	I_0	Reverse saturation current,
P_{losses}	Represents thermal losses in the system (W).	Q	Elementary charge.
p	The pressure (Pa).	n	Ideality factor of the diode.
V	The specific volume (m^3/Kg).	C_{pv}	Thermal capacitance of the PV cell (J/C°).
γ	Gamma is the adiabatic index.	K	Boltzmann constant.
$\dot{m}$	The mass flow rate of the working fluid (Kg/s).	T	Temperature of the PV cell (C°).
h_{inlet}; h_{outlet}	The enthalpies at the turbine's inlet and outlet (J/Kg).	I_{ph}	Photocurrent.
m_{fluid}	The mass flow rate of the heat transfer fluid (Kg/s).	I_d	Diode current.
R_s	Series resistance (Ω).	V	Voltage across the PV cell (V).
Abbreviations		EES	Engineering Equation Solver
IRENA	International Renewable Energy Agency	TES	Thermal energy storage
$s-ORC$	Solar Organic Rankine Cycle	HTF	Heat Transfer Fluid
CSP	Concentrating solar power	*PV*	Photovoltaic
DNI	Direct normal irradiance	*SF*	Solar field
PTC	Parabolic trough collector	*LCOE*	Levelized cost of electricity
PP	Payback period	*PCU*	Power conditioning unit
ORC	Organic Rankine Cycle		

This study compares the implementation of solar energy systems in three regions of Algeria: Adrar, Illizi, and El Bayadh, focusing on the use of CSP-ORC and PV technologies for pumping applications. The selected regions Adrar, Illizi, and El Bayadh each have distinct climatic conditions and solar resources, making them ideal for evaluating the effectiveness of solar technologies. The study aims to assess how CSP-ORC and PV systems can be tailored to enhance water management and support agricultural activities in these areas.

Table 1. CSP-ORC power plants with a power output in the range 50kW-5MW, [3, 8–13].

Plant (date)	Country	Collector type	Collecting area, m^2	HTF	Operating temperature, C°	ORC system (Backup)	Power output	TES type (capacity)
Saguaro power (2006)	USA-AZ	PTC	10340	Xceltherm 600	300/248	Ormat (solar only)	1.00	None
Lafayette (2012)	USA-LA	PTC	01051	Water	121/93	ElectraTherm (solar only)	0.05	Buffer
Airlight energy Baha 2014	Morocco	PTC	06160	Air	570/270	Turboden 18 HR (solar+ waste heat)	2.00	Packed-bed of rochs
Rend-CSP (2014)	Italy	LFC	09780	Mineral Oil	280	N.A (Solar-Biomass)	1.00	None
Tampa (2014)	USA-FL	PTC	01021	Glycol	116/77	ElectraTherm (Solar only)	0.05	PCM
Archimed (2015)	Italy	PTC	08000	Thermal Oil	305/204	Turboden 12 HRS (Gas boiler)	1.00	Direct (1h)
Stillwater Ge-Solar (2015)	USA-NV	PTC	24778	Water	N.A.	Isobutane units (Solar-geothemal)	2 of 35	None
Aalborg CSP-Bronderslev	Denmmark	PTC	26929	N.A.	312/252	Turboden 40 CHPRS split (Solar-biomass)	0.60	None
Ottana solar facility (2017)	Italy	LFC	08592	Thermal oil	275/165	Turboden 6HR Special (solar-only)	1.00	Direct (4.92 h)
IRESEN (under condution)	Morocco	LFC	11400	Mineral oil	300/180	Exergy Organic EPS 150 (solar only)	1.00	Buffer (20 min)
Care Solar Thermal	Morocco	LFC	10000	Water	280/160	N.A.	1.00	Steam Drum (2h)
NOOR ORC Demo 2023	Morocco	PTC	10000	Thermal oil	300/200	Turboden 6HR Special (solar-only)	0.80	None
Indo-Solar Biomass Hybrid Project 2024	India	PTC	10000	Thermal oil	350/210	Solar-biomass	1.00	None

2. Systems description and methodology

We provide details of the configurations of two systems considered in this work, the solar Organic Rankine Cycle (s-ORC) system consists of an ORC power block coupled to a field of solar collectors as shown in Fig. 1. The collectors are of the parabolic trough type, which concentrate solar direct normal irradiation (DNI). The solar field collects thermal energy using HTF, which is transferred to the power block through a heat exchanger (Boiler), In this study, we analyze the s-ORC system. The auxiliary energy consumption of cycle equipment is based on a PV system with batteries providing the necessary energy. On the other hand, we analyze the s-ORC system without considering the auxiliary energy consumption of cycle equipment powered by a PV system. Finally, we compare the s-ORC with power plant photovoltaic output 1MW under the climatic conditions of three regions (Adrar, El-bayadh and Ilizi) in Algeria.The simulation software is from TRNSYS (a program used to simulate solar energy applications; it has been marketed since 1975) [14, 15], and it is a complete and extensible software for simulating transient

systems [16, 17]. It was therefore selected by the authors of the document to develop the simulation model for the installed pilot system. Additionally, the ESS program was integrated with TRNSYS to simulate the Organic Rankine Cycle. Regarding DNI, the Meteonorm program was used.

Table 2. ORC performances at reference conditions [18].

Gross electrical power	1.20 MW
Gross electrical efficiency	25.00 %
Net electrical efficiency	24.00 %
Thermal power input	4.82 MW
Thermal oil inlet / outlet temperature	305 / 206
Auxiliary power consumption	0.05 MW
Cooling water inlet / outlet temperature	25 / 35
Ambient temperature	15.00 C°

2.1 Configuration-one CSP_ORC

2.1.1 Organic Rankine cycle ORC

The growing demand for efficient and sustainable energy solutions has led to the increased adoption of advanced energy systems such as the Organic Rankine Cycle (ORC). Among these technologies, the Turboden 6HRS special is designed to produce a net electric power of 1.16 MW with a net efficiency of 25% under nominal conditions. Table 2 shows the performance of the ORC unit under reference conditions, but the ORC often operates outside from nominal condition as confirmed by the first experimental results [26].

2.2 Configuration-two PV system

The nominal power of the photovoltaic system plant is set at 1 MW.It consists of a field of unmonitored monocrystalline silicon PV modules, a power conditioning unit (PCU), and a battery storage unit. The PCU functions as an interface between the solar field, battery storage, and AC charging.The photovoltaic system, is a small circuit designed to cover the auxiliary power of the ORC and, on the other hand, for comparison purposes with CSP-ORC. The solar photovoltaic field generates continuous electrical energy. The photovoltaic system's batteries store the excess energy provided by the solar field in electrochemical form.

3. Solar energy incidence and efficiency

3.1 Calculation of solar energy incident

3.1.1 Global solar irradiance (DNI)

DNI(t) (Direct Normal Irradiance) represents the direct component of solar energy available per unit area perpendicular to the sun's rays. The total solar energy captured over agiven time period is calculated as Eq. 1, [19]:

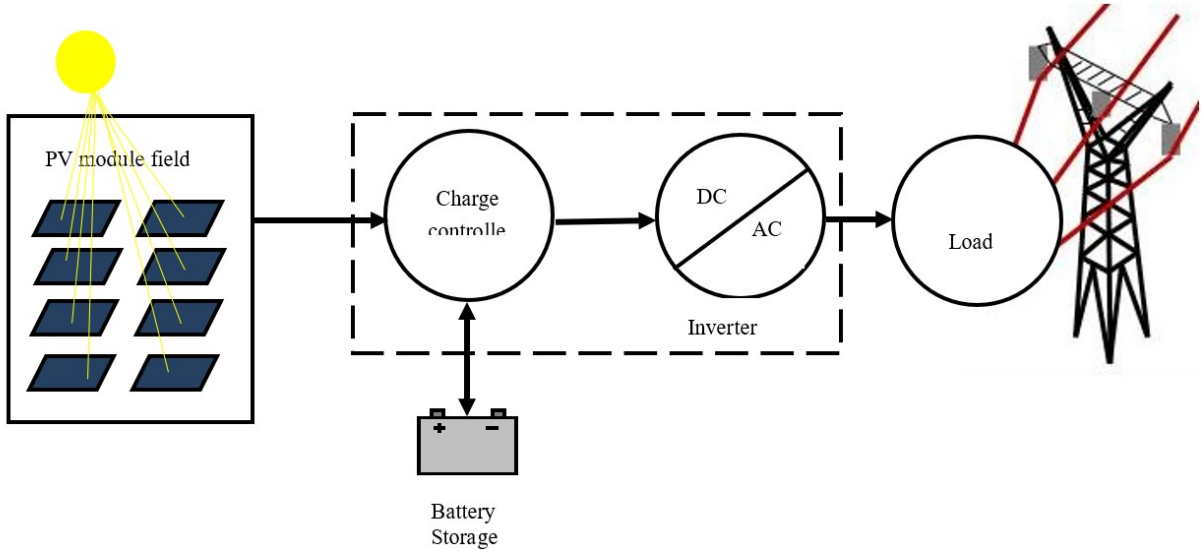

Figure 1. Schematic layout of the PV power plant.

$$E_{solar} = \int DNI(t) \times A_{optique} \times \eta_{optique} \; dt \tag{1}$$

Where $A_{optique}$ the optical aperture area of the solar field (m^2), and $\eta_{optique}$ is the global optical efficiency, accounting for losses due to reflection, absorption, misalignment, and other optical factors.

3.2 Thermal efficiency of the solar field

3.2.1 Thermal power absorbed

The thermal energy collected by the solar field is calculated as Eq. 2, [20].

$$Q_{th} = DNI(t) \times A_{optique} \times \eta_{optique} \times \eta_{thermique} \tag{2}$$

Where $\eta_{thermique}$ is the thermal efficiency of the solar field, which is influenced by thermal losses in the receiver tubes.

3.2.2 Differential equations of the Heat transfer

The heat transfer to the working fluid (HTF) in the solar collectors can be modeled using an energy balance that includes the dynamics of the fluid temperature [21].

3.2.3 Energy balance for the heat transfer fluid

The energy entering the fluid from the solar collectors is given by Eq. 3:

$$\frac{dQ}{dt} = m_{fluid} \times C_{fluid} \times \frac{dT_{fluid}}{dt} \tag{3}$$

Where m_{fluid} is the mass flow rate of the heat transfer fluid, $C_{fluid}$is the specific heat capacity of the fluid, and T_{fluid} the temperature of the fluid.

3.2.4 Differential equation for fluid temperature

The temperature change of the fluid in the collectors can be described by the following differential equation Eq. 4, [21]:

$$m_{fluid} \times C_{fluid} \times \frac{dT_{fluid}}{dt} = Q_{solar} - P_{losses} \tag{4}$$

Where P_{losses} represents thermal losses in the system (due to conduction, convection, radiation). These losses can be modeled by Eq. 5.

$$P_{losses} = U_{losses} \times A_{exposed} \times (T_{fluid} - T_{amb}) \tag{5}$$

where $A_{exposed}$ is the exposed surface area for heat losses, T_{amb} is the ambient temperature, and U_{losses} is the heat transfer coefficient.

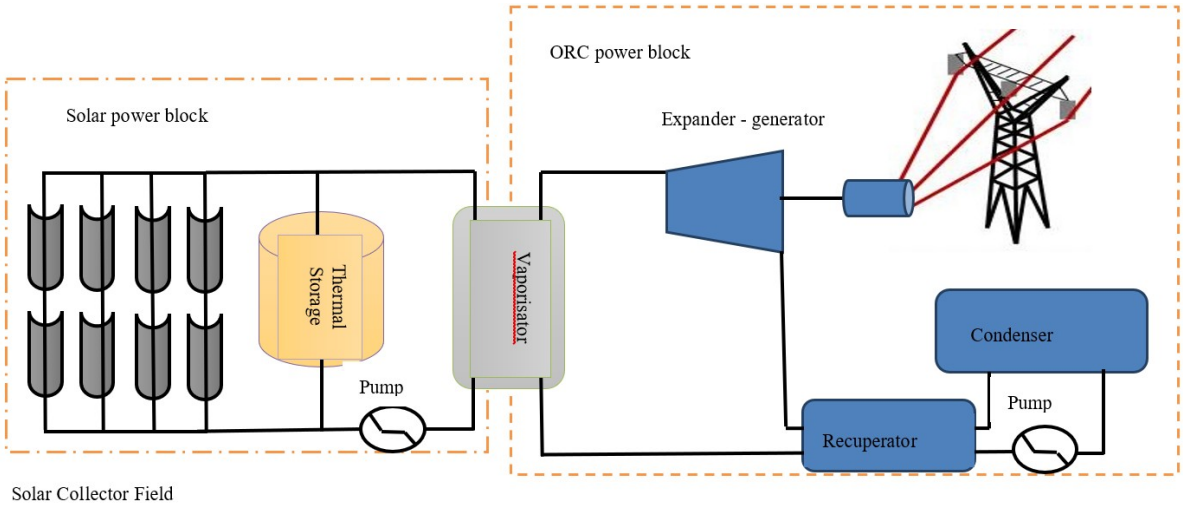

Figure 2. Schematic layout of Configuration 1 for the CSP-ORC plant.

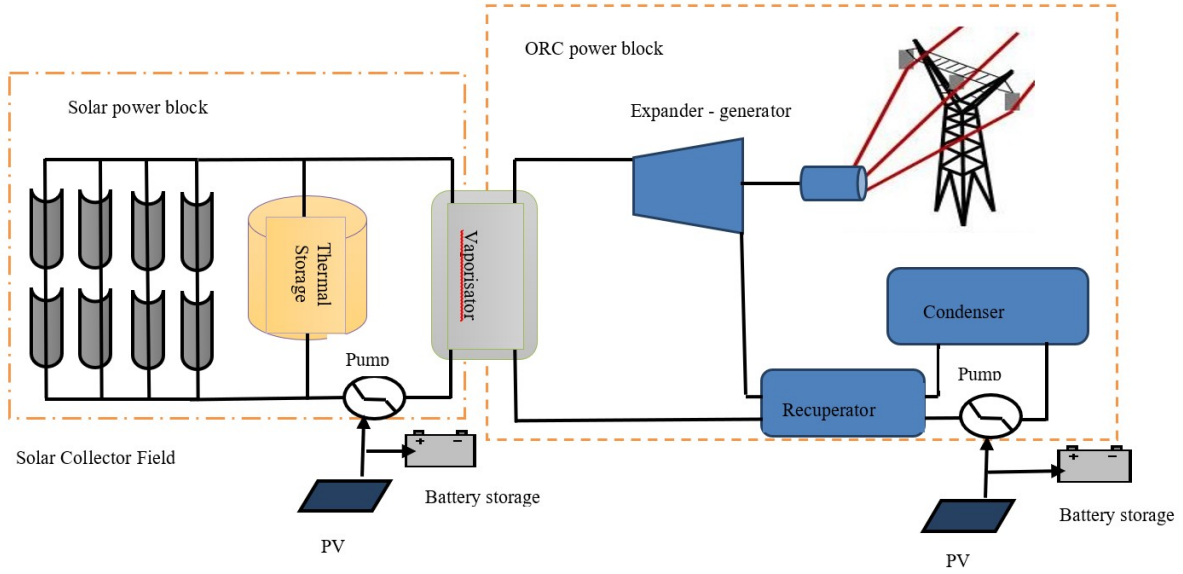

Figure 3. Schematic layout of Configuration 2 for the CSP-ORC plantt.

4. Mechanical power of the ORC

4.1 Heat-to-work conversion

The heat energy collected is converted into mechanical power in the Organic Rankine Cycle (ORC) system as Eq. 6, [20, 22, 23].

$$P_{mec} = Q_{th} \times \eta_{ORC} \tag{6}$$

Where η_{ORC} is the thermal-to-mechanical conversion efficiency of the ORC. It depends on the high and low operating temperatures and is approximately given by the Carnot efficiency Eq. 7.

$$\eta_{ORC} = 1 - \frac{T_{cond}}{T_{source}} \tag{7}$$

Where T_{source} is the temperature of the thermal fluid exiting the solar receivers, T_{cond} is the condensation temperature of the ORC working fluid.

4.2 Energy balance for the turbine

The turbine converts thermal energy into mechanical work. The work produced by the turbine is the change in enthalpy of the working fluid between the inlet and the outlet, Eq. 8 [24].

$$W_{turbine} = \dot{m} \times (h_{inlet} - h_{outlet}) \tag{8}$$

Where $\dot{m}$ is the mass flow rate of the working fluid and h_{inlet} and h_{outlet} are the enthalpies at the turbine's inlet and outlet. The enthalpy of the working fluid depends on temperature and pressure. If the turbine operates at constant pressure, the change in enthalpy can be modeled as Eq. 9.

$$\frac{dQ}{dt} = \dot{m} \times \frac{dh}{dt} \tag{9}$$

The enthalpy change is typically related to temperature and pressure using equations of state for the working fluid.

4.3 Energy balance for the condenser

The condenser cools and condenses the working fluid. The process can be modeled as an adiabatic or isothermal compression, resulting in a pressure and temperature increase of the working fluid. The equation for the energy in the compressor is Eq. 10 [24].

$$\frac{dQ}{dt} = \dot{m} \times (h_{inlet} - h_{outlet}) \tag{10}$$

In the case of adiabatic compression, this process can be modeled using the first law of thermodynamics. The differential equation for the adiabatic compression process is Eq. 11.

$$p.V^{\gamma} = c^{st} \tag{11}$$

Where p is a pressure, V is a specific volume, and γ is an adiabatic index.

4.4 Overall Efficiency of the System

4.4.1 Global efficiency

The overall system efficiency, which combines the efficiencies of all subsystems, is expressed as Eq. 12 [25].

$$\eta_{global} = \frac{P_{elec}}{E_{solar}} \tag{12}$$

Where P_{elec} is the net electrical power output, accounting for internal consumption by pumps, fans, and other auxiliary components, and E_{solar} is the total solar energy incident on the system.

5. Mathematical model for a PV system

Photovoltaic (PV) systems convert solar radiation into electrical energy. A mathematical model based on differential equations can describe the dynamic behavior of a PV system, accounting for changes in solar irradiance, temperature, and electrical load [18, 26].

5.1 Electrical model of a PV cell

The output current (I) of a PV cell can be described using the single-diode model Eq. 13.

$$I = I_{ph} - I_d - \frac{V + (R_s \times I)}{R_{sh}} \tag{13}$$

Where I_{ph} is photocurrent (depends on solar irradiance), I_d is diode current, V is the voltage across the PV cell, R_s is the series resistance, and R_{sh} is the shunt resistance. The diode current I_d is given by the Shockley diode equation Eq. 14.

$$I_d = I_o \times e^{q\frac{V+R_s.I}{n.k.T}} - 1 \tag{14}$$

Where I_o is the Reverse saturation current, q is the elementary charge, n is the ideality factor of the diode, k is Boltzmann constant, and T is the temperature of the PV cell.

Table 3. Assumed performance values for different components of the PV system [27, 28].

Component	Estimated Cost
Solar Field Investment Cost	200 €/m^2
Power Block Investment Cost (ORC System)	1000 €/kW
Thermal Storage System Investment Cost	30 €/kWh of storage capacity
Various Costs	15% of the total investment
Annual Operation & Maintenance (O&M)	1% of CAPEX per year
Lifetime	25 years
Interest Rate	6 %
Electricity Selling Price (Ps)	0.11 €/kWh

5.2 Thermal dynamics

The temperature of the PV cell changes due to solar heating and heat dissipation. The temperature dynamics can be described by an energy balance Eq. 15:

$$C_{pv} \times \frac{dT}{dt} = G \times (1 - \eta_{pv}) \times A_{PV} - h \times A_{pv}(T - T_{amb}) \tag{15}$$

Where C_{pv} is the thermal capacitance of the PV cell, η_{pv} the electrical efficiency of the PV cell, A_{PV} the surface area of the PV panel, h the heat transfer coefficient and T_{amb} is the ambient temperature.

5.3 Electrical Power Output

The power output P of the PV system is Eq. 16:

$$P = V.I \tag{16}$$

The voltage V and current I are dynamically influenced by load and irradiance, and their relationships can be described by the above differential equations.

6. Economic analysis

6.1 Levelized cost of electricity

The LCOE is a key metric used to evaluate the economic feasibility of a photovoltaic (PV) power plant. It represents the average cost per unit of electricity produced over the system's lifetime, considering all associated costs. The LCOE can be calculated using the following formula Eq. 17 [29–31].

$$LCOE = CAPEX + OPEXt + REPEXt/Et \tag{17}$$

where $CAPEX$ refers to the initial investment cost, $OPEXt$ represents the annual operational and maintenance costs at year t, and $REPEXt$ accounts for periodic replacement costs (inverter replacement after 10–15 years). The denominator, Et, corresponds to the total electricity generation (kWh) over the system's operational lifetime, typically 25 years. Annual electricity production for the PV system: Adrar: 2.65$GWh/year$ *Illizi* : 2.76$GWh/year$ El Bayadh: 2.39$GWh/year$.

6.2 Calculation of payback period (PP)

PP represents the time needed to recover the initial investment cost Eq. 18 [32].

$$PP = Initial\ Investment\ Cost/Annual\ Savings \tag{18}$$

If electricity is sold at a price Ps, then Eq. 19:

$$AnnualRevenue = E \times Ps \tag{19}$$

For a CSP-ORC system, the LCOE is calculated similarly to other energy systems, but it must account for additional factors such as the thermal storage system, heat transfer fluids, and the efficiency of the ORC cycle [33]. Annual electricity production for the CSP-ORC system: Adrar: 4.15$GWh/year$, *Illizi* : 4.2$GWh/year$, El Bayadh: 3.8$GWh/year$.

Table 4. Assumed performance values for different components of the CSP-ORC system [34, 35].

Component	Values
Investment Cost of PV panel	4 €/Wp
Investment Cost of the frame	0.4 €/Wp
Investment Cost of the inverter	0.1 €/W
Various costs	15% of total investment cost
Yearly O&M cost (% CAPEX)	1%
Lifetime	25 years
Interest rate	6%
Electricity Selling Price (Ps)	€0.11/kWh

7. Results and discussion

7.1 Validation of numerical results

The proposed system, which consists of a CSP-ORC and PV, was validated by verifying each component. Figure 4 presents a comparison between the current numerical results and those obtained by Mario Petrollese and Daniele Cocco with respect to the ORC. The figure demonstrates excellent agreement, with a percentage deviation ($'e'$) between the numerical results of the current study and those of Mario Petrollese and Daniele Cocco ranging from 0.2% to 0.4%.

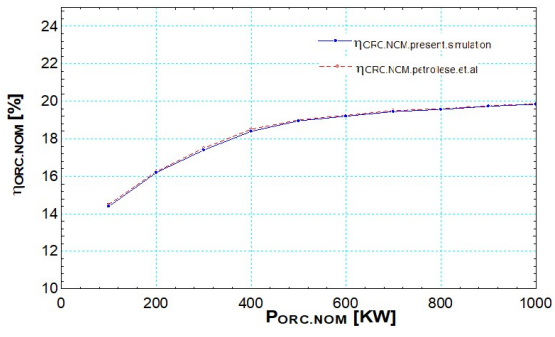

Figure 4. Comparison between the current numerical results and those obtained by Mario Petrollese and Daniele Cocco.

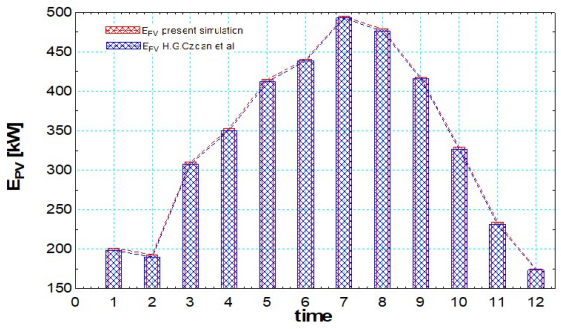

Figure 5. Compares the present study with the study conducted by H.G. Ozcan et al.

Similarly, Fig. 5 compares the present study with the study conducted by H.G. Ozcan et al. on solar panels. The results show very good compatibility between the two studies. Finally, the CSP component was validated results obtained by Dudley V.E. et al. and the present simulation performed using the TRNSYS software, as shown in Fig. 6. Therefore, the numerical model effectively simulates the proposed ORC system and serves as a reliable tool for predicting its performance under various operating conditions, enabling the identification of optimal locations for deploying this system. The consistent results between the two studies emphasize the importance of ongoing research in improving the efficiency of the Organic Rankine Cycle. Future research should explore other factors, such as the quality of the working fluid and varying operating conditions, on performance. Additionally, comparative studies using different types of heat sources should be conducted to better understand their impact on efficiency

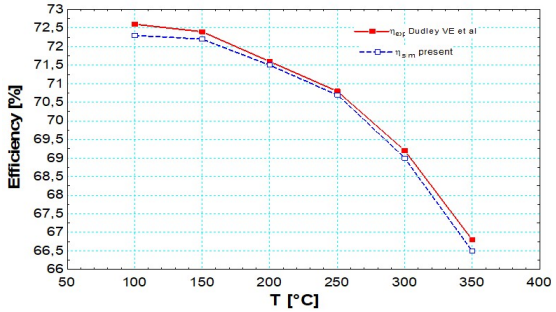

Figure 6. Compares the present study with the study conducted by Dudley V.E. et al.

7.2 Efficiency of the CSP-ORC solar plant in the regions of Adrar

On March 21, the efficiency of the CSP-ORC solar plant in the regions of Adrar, El Bayadh, and Illizi shows positive results. When solar panels are added to power the pump, an improvement in efficiency is observed when comparing performance with and without integration. The efficiency increases noticeably around 9 AM, peaks between 12 PM and 2 PM, then gradually declines until around 4 PM, eventually dropping to very low levels by the end of the day.

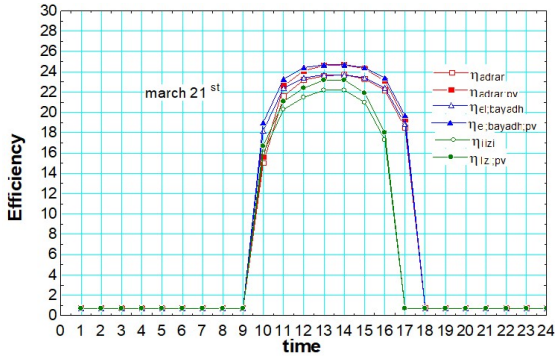

Figure 7. Daily performance trend of the plant on March 21 in Adrar, Illizi, and El Bayadh.

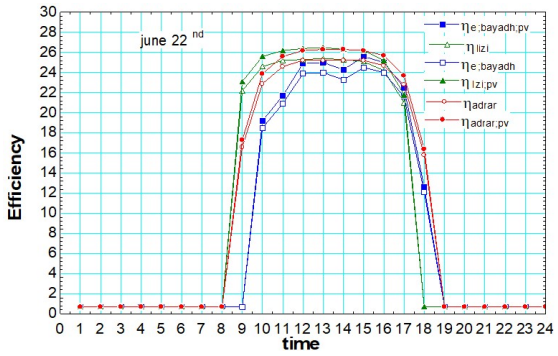

Figure 8. Daily performance trend of the plant on June 22 in Adrar, Illizi, and El Bayadh.

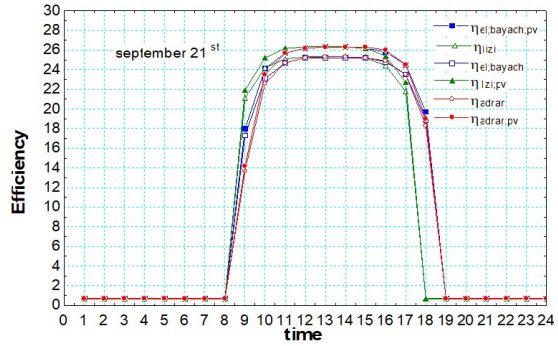

Figure 9. Daily performance trend of the plant on September 21 in Adrar, Illizi, and El Bayadh.

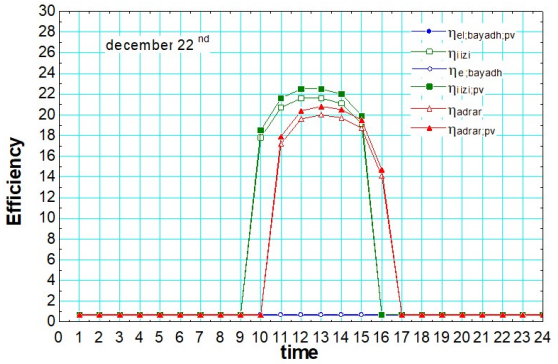

Figure 10. Daily performance trend of the plant on December 22 in Adrar, Illizi, and El Bayadh.

Efficiency begins to rise around 8 AM, peaks shortly after 11 AM, and remains stable until about 3 PM, reflecting the longer daylight hours near the summer solstice. In Adrar, the difference in efficiency between configurations CSP with and without photovoltaic (PV) panels is minimal, suggesting that local conditions, such as high temperatures or dust, limit the impact of solar panels. Conversely, El Bayadh shows a noticeable improvement in efficiency when solar panels are used, indicating that solar energy significantly enhances performance in this region. The most pronounced improvement is observed in Illizi, where the addition of solar panels makes the region highly favorable for solar energy generation. Overall, efficiency on June 22 is higher than in March, primarily due to increased solar irradiance and extended daylight hours during the summer months. Efficiency in the three regions follows a similar pattern to previous months, with a peak between 11 AM and 3 PM. 1. Adrar: There is a slight improvement in efficiency with PV, but the difference remains small, suggesting that local conditions limit the effectiveness of solar panels in this region.

2. El Bayadh: Efficiency shows a significant improvement with PV, highlighting favorable conditions for solar energy use.

3. Illizi: The use of solar panels significantly boosts efficiency, indicating that Illizi is well-suited for solar energy generation.
Efficiency in September is lower than in June due to a decrease in solar irradiance as autumn approaches. However, Illizi continues to benefit the most from PV, followed by El Bayadh, with Adrar showing the least improvement. The graph for December 22 shows the absence of results for El Bayadh. Adrar: There is a slight improvement in efficiency with PV, but the difference is not significant. El Bayadh: There is no efficiency with the use of PV, suggesting that local conditions may limit their effectiveness. Illizi: Efficiency with PV is significantly enhanced, making Illizi the region most suited for solar energy generation even in winter. Efficiency in December is lower in Illizi and Adrar compared to September, and there is no efficiency in El Bayadh, due to the decrease in solar irradiance as winter approaches. However, Illizi continues to benefit the most from PV. The results show that solar panel efficiency varies significantly by region and season. Illizi is consistently the most favorable region for solar energy, followed by El Bayadh, while Adrar benefits the least. These findings highlight the need for tailored strategies to optimize solar energy use, considering regional differences and seasonal variations in solar availability.

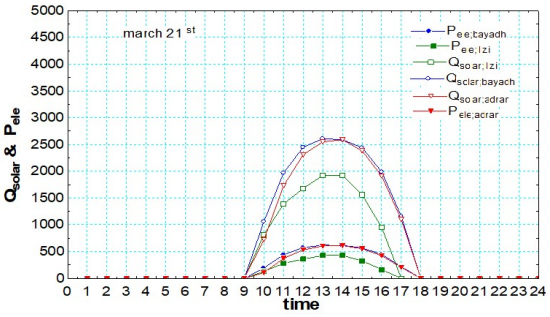

Figure 11**.** Variation of electric power and solar power on march 21 in: Adrar, Illizi, and El Bayad.

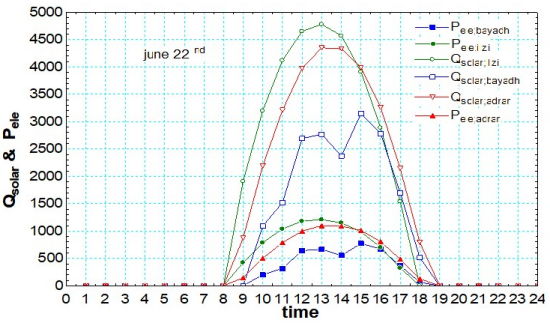

Figure 12**.** Variation of electric power and solar power on June 22 in: Adrar, Illizi, and El Bayadh.

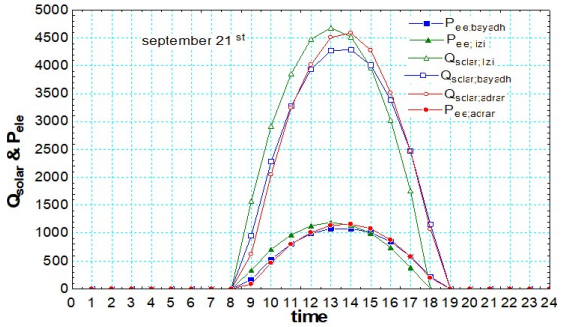

Figure 13**.** Variation of electric power and solar power on September 21 in: Adrar ,Illizi and El Bayadh.

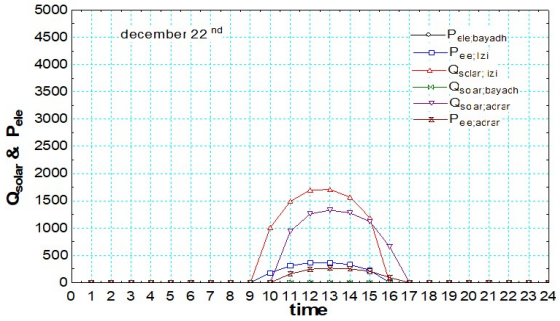

Figure 14**.** Variation of electric power and solar power on December 22 in: Adrar ,Illizi and El-Bayadh.

The graph shows the power electric and solar power over time on March 21 for three regions in Algeria: El Bayadh, Illizi, and Adrar. Each region has different markers and line colors representing various measurements: Both the power electric and solar energy collection reach their peaks around midday (12:00 to 13:00), reflecting the sun's highest intensity. El Bayadh shows the highest power generation among the three regions, followed by Illizi and Adrar. This graph suggests that El Bayadh has the most favorable conditions or systems for solar power generation on March 21, as indicated by both the higher power electric output and solar thermal energy collection. Illizi follows, while Adrar shows comparatively lower power output, possibly due to different solar intensity or system efficiency in this region. This graph illustrates power electric and solar thermal energy on June 22 for the same three regions in Algeria (El Bayadh, Illizi, and Adrar). Overall Increase in Solar thermal Energy Collection and Power electric Generation, Compared to March 21, the energy collected and power generated in all regions on June 22 are noticeably higher. This aligns with higher solar irradiance during summer. Adrar shows the highest peak in solar energy collection around noon, followed by El Bayadh and Illizi. This pattern is different from the March graph, where El Bayadh had higher energy collection. Adrar's power generation reaches the highest peak, surpassing El Bayadh and Illizi, which is a significant shift compared to the March 21 data. El Bayadh, which had the highest output in March, shows lower power output than Adrar but remains higher than Illizi. Adrar's solar energy collection and power output peak sharply around midday and decline rapidly, which is typical in regions with intense solar exposure and quick temperature rises. Illizi and El Bayadh have a more moderate peak, with the curve rising and falling more gradually. The graph depicts power and solar thermal energy values on September 21 across three Algerian regions: El Bayadh, Illizi, and Adrar. All regions exhibit peak power and energy collection around midday (12:00-13:00), aligning with the sun's trajectory. Illizi achieves the highest power generation and solar energy collection, indicating optimal solar resource availability or system efficiency, followed by El Bayadh, which outperforms Adrar. Adrar shows the lowest performance, consistent with its output in March but contrasting with its strong summer performance in June. The curves display sharp, symmetrical patterns, suggesting stable solar conditions with minimal daily variability. Overall, Illizi demonstrates superior performance, while El Bayadh remains productive, and Adrar experiences notable seasonal variation. These observations underscore the importance of tailoring renewable energy technologies to regional and seasonal solar conditions in Algeria's arid zones. On December 22, power output in all regions of Algeria—El Bayadh, Illizi, and Adrar—peaks around midday (11:00 - 14:00), coinciding with the highest levels of solar irradiance, a typical pattern for solar-based systems. Electrical power (P) shows regional variations, with each region producing different outputs due to factors such as solar irradiance and system efficiency. Solar thermal power (Q) values, however, differ significantly, with Illizi reaching the highest thermal output, followed by El Bayadh and Adrar, indicating that CSP-ORC systems in Illizi have the greatest potential for capturing solar energy. The comparison between CSP-ORC and PV systems reveals that CSP-ORC systems (represented by Q) capture more solar energy but convert less of it into electrical power than PV systems, which show relatively lower electrical power outputs on this day. The performance of both systems is influenced by the season, as the lower solar angles in winter reduce energy capture efficiency. This highlights the regional and seasonal variations in solar power generation across Algeria's arid zones, suggesting that CSP-ORC systems offer advantages for thermal energy capture even during winter months.

7.3 Configuration-two

In this proposed arrangement, the curves showed acceptable results in raising the value of the electrical energy produced by 40 kW. The graph shows the electrical power output (P) on March 21 for El Bayadh, Illizi, and Adrar, comparing systems with photovoltaic (PV) integration for pumping and those without PV. Power output peaks around midday (11:00 - 14:00) in all regions, which is typical for solar-based systems. PV-integrated systems show a slight increase in power output compared to those without PV, especially in El Bayadh and Adrar, where the output reaches higher values at midday. While Illizi benefits from PV integration, its overall energy production remains lower than that of El Bayadh and Adrar, likely due to less favorable solar conditions or differences in system design. Compared to winter, the spring equinox in March provides more balanced sunlight, resulting in a more symmetrical power output curve. Overall, the integration of PV systems improves electrical power production, with El Bayadh and Adrar showing greater benefits, highlighting the effectiveness of PV systems in boosting energy output in Algeria's arid regions.

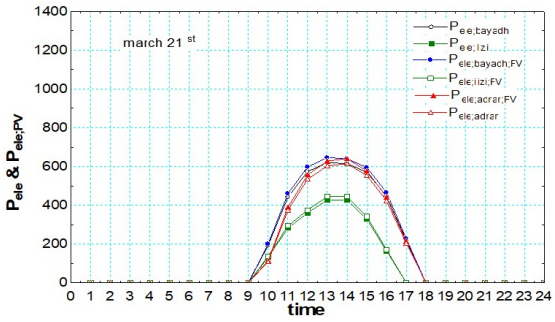

Figure 15**.** The produced thermal and electrical power is affected by the evolution of direct normal irradiation throughout the day on March 21 in Adrar, Illizi, and El Bayadh.

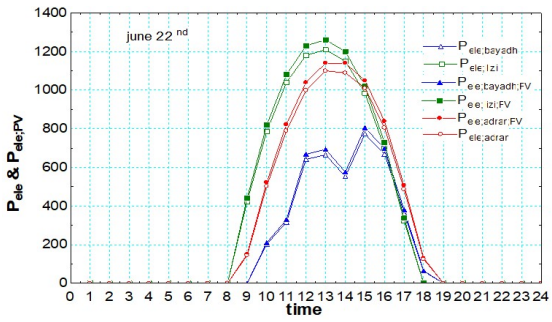

Figure 16**.** The produced thermal and electrical power is affected by the evolution of direct normal irradiation throughout the day on June 22 in Adrar, Illizi, and El Bayadh.

This graph displays the electrical power output (P) on June 22 for three regions: El Bayadh, Illizi, and Adrar, comparing systems with and without photovoltaic (PV) integration for pump feeding. Power output in all regions peaks around midday (11:00 to 14:00), reflecting the effects of the summer solstice, with the longest daylight hours and the highest solar elevation angle of the year. Systems integrated with PV show increased output, with Illizi reaching the highest production level when PV is integrated, suggesting favorable solar conditions or enhanced system performance during the summer. El Bayadh also shows a notable increase in output with PV, especially during peak hours. Adrar benefits from PV integration as well, but to a lesser extent, indicating moderate solar irradiance or system performance. The summer solstice, with its extended daylight hours and high solar angles, contributes to the increased and broader power output curve, particularly for PV-enhanced systems. Overall, the integration of PV systems significantly boosts power generation, especially in Illizi and El Bayadh, highlighting the potential of PV systems in enhancing energy production in Algeria's arid regions during periods of high solar irradiance, such as summer. This graph illustrates the electrical power output (P) on September 21 for three regions: El Bayadh, Illizi, and Adrar. It compares systems with and without photovoltaic (PV) integration for pump feeding. In all regions, power output peaks around midday (from 11:00 to 15:00), reflecting the effects of the summer solstice, which brings the longest daylight hours and the highest solar elevation angle of the year. The PV-enhanced systems show a significant increase in power production. Illizi achieves the highest output when PV is integrated, indicating favorable solar conditions or enhanced system performance. El Bayadh also experiences a notable increase in power, especially during peak hours. Adrar benefits from PV integration as well, but to a lesser extent, suggesting moderate solar irradiance or system efficiency. Overall, the summer solstice, with its extended daylight hours and high solar angles, leads to a wider power output curve, particularly for PV systems. The integration of PV systems notably boosts power generation, especially in Illizi and El Bayadh, highlighting the potential of PV systems to improve energy production in Algeria's arid regions during high solar irradiance periods like summer. The graph compares the electrical power generated by the solar power plant with an optimized Organic Rankine Cycle (ORC) system, which includes solar panels to power the pump, and the electrical power generated by the solar power plant with a conventional Organic Rankine Cycle (ORC) system on December 22. The absence of results for Adrar is due to low solar irradiance during this period, leading to no power generation. For the other regions, such as El Bayadh and Illizi, the optimized system shows better performance compared to the non-optimized system, especially during peak solar hours, indicating a better utilization of the available solar energy in these regions.

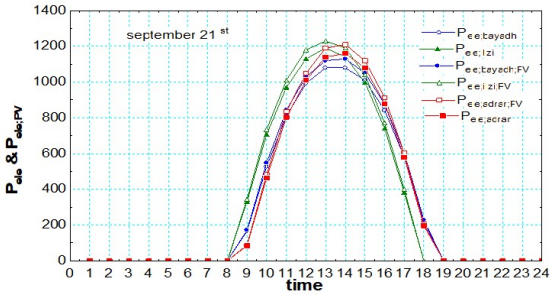

Figure 17**.** The produced thermal and electrical power is affected by the evolution of direct normal irradiation throughout the day on September 21 in Adrar, Illizi, and El Bayadh.

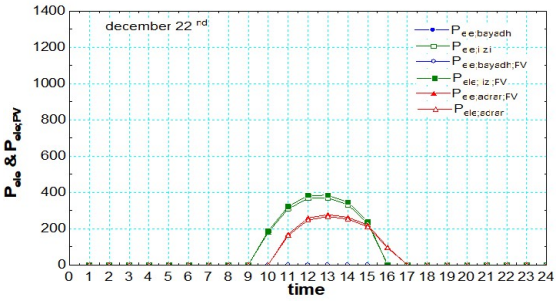

Figure 18**.** The produced thermal and electrical power is affected by the evolution of direct normal irradiation throughout the day on December 22 in Adrar, Illizi, and El Bayadh.

7.4 Efficiency of a photovoltaic (PV)

This histogram compares two energy values, electrical energy and solar energy, across the months of the year in the Illizi region. The values exhibit seasonal variation, peaking between May and August due to increased solar irradiance in summer and declining during the winter months. The significant difference between the two values highlights the seasonal nature of energy production and the potential to improve system efficiency for better energy utilization. The line graph illustrates energy trends across three locations in Algeria: Adrar, Illizi, and El Bayadh, over the months of the year. The values represent the generated electrical energy and solar energy for each site, showing seasonal variation with peaks during the summer months (May to August) and declines in winter. Illizi consistently exhibits the highest energy values, indicating favorable conditions for energy production, while Adrar and El Bayadh display similar patterns with slightly lower values. Thermal energy values exceed electrical energy values at all sites, highlighting potential losses in energy conversion

or utilization. Overall, Illizi is the most efficient site, with opportunities to enhance energy utilization efficiency across all locations. The graph compares the efficiency of a photovoltaic (PV) system over a single day (March 21) in three Algerian regions: Adrar, Illizi, and El Bayadh. Efficiency rises rapidly in the morning, stabilizes around midday, and declines sharply after sunset. Illizi and Adrar demonstrate nearly identical and superior efficiency levels, indicating favorable solar conditions. In contrast, El Bayadh exhibits slightly lower performance, likely due to regional climatic differences. Overall, while all three regions are suitable for PV installations, Adrar and Illizi show a marginal advantage, particularly during peak solar hours.

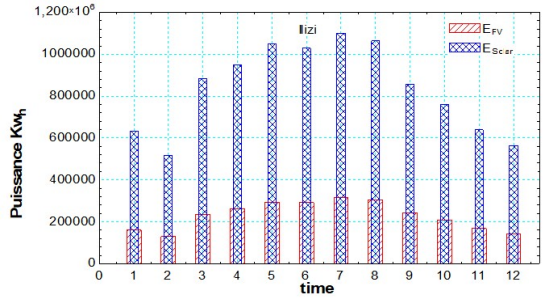

(a) Illizi

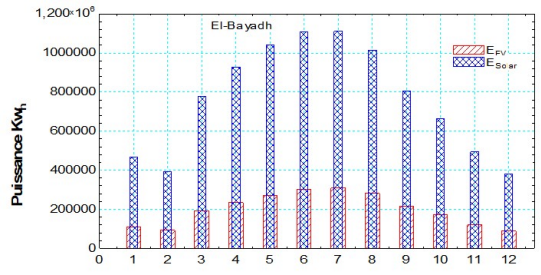

(b) El Bayadh

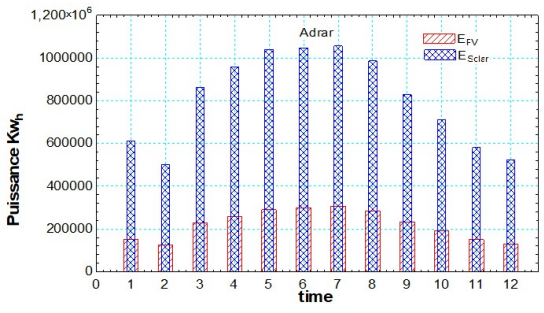

(c) Adrar

Figure 19. (a),(b) and (c) Comparison of electrical energy and solar energy of the photovoltaic solar plant throughout the year in three locations.

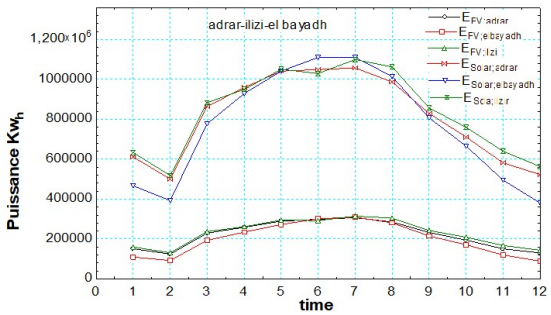

Figure 20. Variation of electrical power of the photovoltaic solar plant throughout the year.

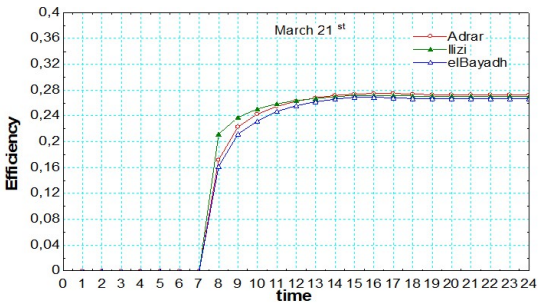

(a) March 21

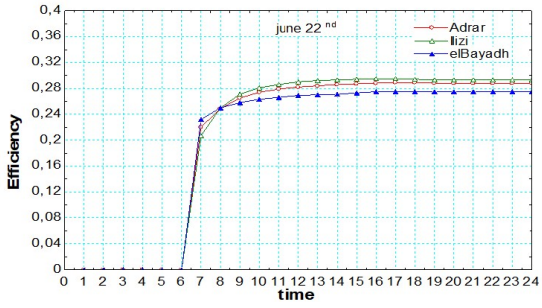

(b) June 22

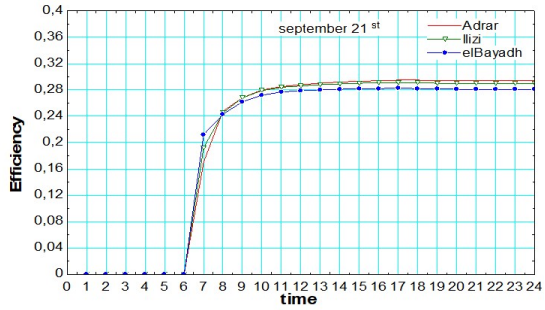

(c) September 21

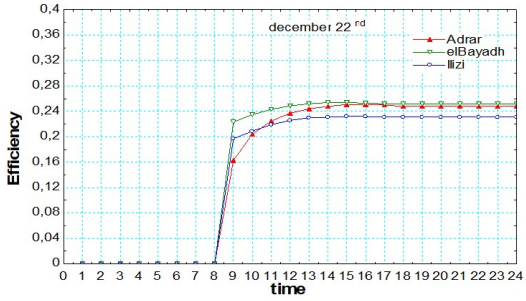

(d) December 22

Figure 21. Daily performance trend of the PV plant in Adrar, Illizi, and El Bayadh.

The graph shows the efficiency of photovoltaic (PV) systems on December 22 in three Algerian regions: Adrar, El Bayadh, and Illizi. Efficiency rises after sunrise, stabilizes midday, and drops to zero at sunset. El Bayadh exhibits the highest efficiency throughout the day, making it the most favorable location for PV systems during winter. Adrar follows closely, with slightly lower performance. Illizi consistently shows the lowest efficiency, likely due to regional climatic factors or reduced solar irradiance. Overall, the analysis highlights El Bayadh's advantage for solar energy production during this winter period.

7.5 Compared PV & ORC_CSP

Figure 22 presents the annual electrical power output (8760 hours) of Concentrated Solar Power (CSP) and Photovoltaic (PV) systems in the arid regions of Algeria, specifically Adrar, El Bayadh, and Illizi. The graphs show seasonal variations in energy production, with output peaking mid-year (summer) and

decreasing during winter, reflecting the influence of seasonal solar irradiance.

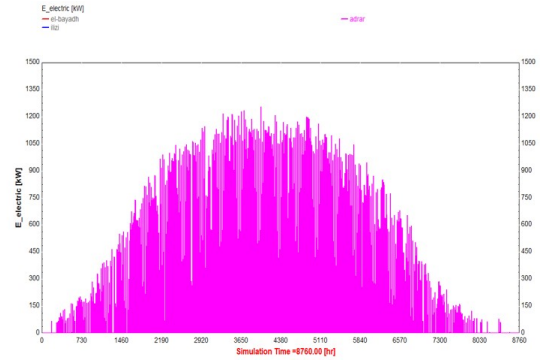

(a) the PV power plant

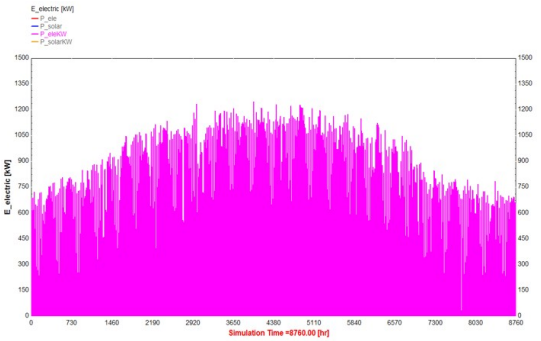

(b) the CSP-ORC plant

Figure 22**.** Evolution of the electricity produced throughout the year by (a) the PV power plant and (b) the CSP-ORC plant.

A daily pattern is also evident, with production rising during daylight hours and ceasing at night, reaching peaks of approximately 1500 kW during summer. When comparing different configurations of CSP and PV systems, both exhibit similar seasonal trends but differ in their response to solar conditions. CSP systems show fewer fluctuations and higher efficiency in areas with high Direct Normal Irradiance (DNI), while PV systems are simpler but less efficient at elevated temperatures. Both systems reach a peak output of around 1500 kW, facilitating the comparison of annual performance and efficiency. The study highlights CSP systems' suitability for providing stable energy in arid regions, while PV systems are more economical and straightforward. It emphasizes the importance of evaluating annual performance to determine the effectiveness of these systems. The curves illustrate in Fig. 7 shows the evolution of the power electric generate during one day, we took four different days of the year (21st march, 22nd june, 21st September and 22nd December) to notice the difference between the electrical energy produced in the Ilizi region, examine performance outside of peak sunlight hours. This graph shows the power output (Pe) of both Concentrated Solar Power and Photovoltaic systems in Adrar, Algeria, throughout the days. Both systems follow a bell-shaped curve, peaking at midday when solar irradiance is highest. PV systems reach higher maximum outputs compared to CSP systems, indicating they may be more efficient under Adrar's solar conditions, especially during midday. Different configurations show better performance with higher peak outputs and steeper curves, suggesting improved efficiency or larger-scale setups. Although CSP systems have lower maximum power outputs, they may offer benefits in thermal energy storage, providing reliability during non-peak hours when paired with appropriate storage systems. Overall, PV systems seem more suitable for meeting midday power demands, while CSP could complement them in a hybrid system to leverage thermal storage. The graph illustrates the evolution of the electric power generated by Concentrated Solar Power (CSP) systems with various configurations and Photovoltaic (PV) systems in the Illizi region, Algeria, during the days of March 21, June 22, September 21, and December 22. Both technologies follow a bell-shaped curve, peaking at midday. However, PV systems outperform CSP in terms of maximum power output, particularly in the more efficient configurations such as December 22 and September 21. CSP configurations also show improved performance with more advanced setups, as seen in December 22. PV systems appear more suitable for maximizing production during peak sunny hours, while CSP systems, despite lower peak performance, can be advantageous due to their thermal storage capabilities, ensuring power generation continues after sunset.

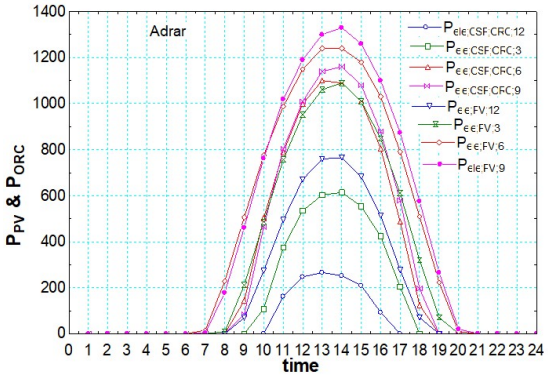

(a) Adrar

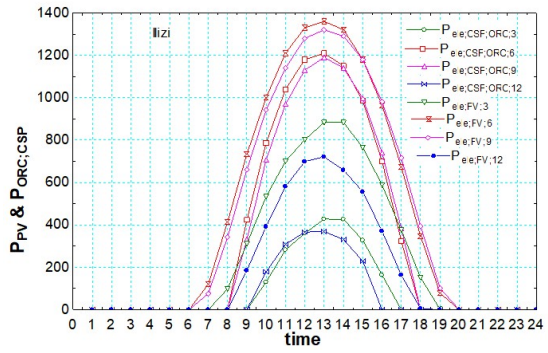

(b) Illizi

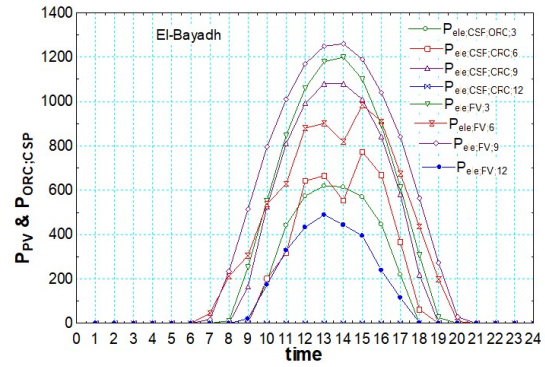

(c) El Bayadh

Figure 23**.** Comparison of the electrical energy generated by the CSP-ORC and PV systems over four days in three locations.

A hybrid approach could therefore achieve optimal energy efficiency in this region. This graph shows the power output of a range of Concentrated Solar Power (CSP) and Photovoltaic (PV) systems throughout the days of March 21, June 22, September 21, and December 22 in the region of El Bayadh, in Algeria. The power output in both CSP and PV systems indicates differences in system design or capacity. Both systems follow a bell-shaped curve, with a peak at midday, but CSP systems outperform PV systems significantly. December records the highest power output, followed by September, then June and March, showing a direct relationship between the system size or efficiency and performance level. Similarly, PV systems perform better with higher numbers, with December ranking first, but they still have lower efficiency compared to CSP. The dominance of CSP systems in El Bayadh reflects their alignment with the region's environmental and solar conditions, benefiting from the intensity of direct sunlight. Although PV systems perform less well compared to CSP, they can serve as a complementary source in hybrid systems to enhance stability and reduce dependence on CSP during periods of lower sunlight.

This analysis highlights CSP systems' suitability for the solar conditions in El Bayadh, making them the optimal choice to meet midday energy demand, with PV as an additional source for stability, Table 5.

Table 5. Comparison of LCOE and payback period for PV and CSP-ORC systems across different sites.

Site	LCOE (€/kWh) PV.	PP (Years) PV.	LCOE (€/kWh) CSP-ORC.	PP (Years) CSP-ORC
Illizi	0.0311	3.62	0.0860	9.52
Adrar	0.0323	3.77	0.0871	9.64
El Bayadh	0.0359	4.18	0.0951	10.53

7.6 The economic analysis

7.6.1 Photovoltaic system

Illizi is the most cost-effective site, with the lowest LCOE (0.0311 €/kWh), ensuring the cheapest electricity production, and the shortest payback period (3.62 years), making it the best investment option. Adrar follows closely, being slightly less efficient but still highly competitive, with an LCOE of 0.0323 €/kWh and a payback period of 3.77 years. In contrast, El Bayadh has the weakest performance, featuring the highest LCOE (0.0359 €/kWh) and the longest payback period (4.18 years), likely due to lower annual electricity production.

7.6.2 CSP_ORC System

Illizi demonstrates the best performance among the three sites, with the lowest LCOE (0.0860 €/kWh), ensuring the most cost-effective electricity production. It also has the shortest payback period (9.52 years), making it the most attractive investment. Adrar follows closely behind, with an LCOE of 0.0871 €/kWh and a payback period of 9.64 years, indicating slightly lower efficiency than Illizi but still a competitive option. In contrast, El Bayadh has the highest costs and the longest payback period, with an LCOE of 0.0951 €/kWh and a payback period of 10.53 years, making it the least favorable site for investment. Comparison of PV and CSP-ORC Systems in Algeria.

8. Conclusion

This study underscores the importance of harnessing solar energy for electricity generation, particularly in isolated and arid regions of Algeria. By comparing the Concentrated Solar Power system with Organic Rankine Cycle (CSP-ORC) and the Photovoltaic (PV) system, valuable insights into the performance of each system under different environmental conditions have been presented. The results indicate that the PV system exhibits superior performance, especially during the colder months, making it an attractive option for meeting energy needs in remote areas. While the CSP-ORC system shows promising potential, it requires further enhancements, such as integrating energy storage systems or utilizing hybrid solutions, to improve its effectiveness and reliability throughout the year. These findings open avenues for future research, where hybrid configurations or alternative energy storage solutions could be explored to bolster the performance of the CSP-ORC system during periods of low solar irradiance. This would contribute to providing sustainable and reliable energy sources, thereby enhancing economic and social development in Algeria's remote areas. In summary, the study reflects the significant potential of solar energy as a sustainable solution for addressing energy needs, emphasizing the importance of ongoing research and development to maximize the benefits of these natural resources. The economic analysis highlights the cost-effectiveness of PV systems, which have lower investment and maintenance costs, as well as a lower LCOE compared to CSP-ORC. The PV system in Illizi achieves the lowest LCOE, while CSP-ORC records the highest in El Bayadh. From an environmental perspective, PV reduces CO_2 emissions by 55.2 tons in Illizi, whereas CSP-ORC prevents 84 tons due to its higher electricity generation. Both systems significantly reduce emissions compared to diesel generators, reinforcing their sustainability.

Authors' contribution

All authors contributed equally to the preparation of this article.

Declaration of competing interest

The authors declare no conflicts of interest.

Funding source

This study didn't receive any specific funds.

Data availability

The data that support the findings of this study are available from the corresponding author upon reasonable request.

REFERENCES

[1] IRENA, "Global energy transformation: A roadmap to 2050," *International Renewable Energy Agency*, 2019 edition. [Online]. Available: www.irena.org/publications

[2] P. N. Botsaris, A. G. Pechtelidis, and K. A. Lymperopoulos, "Modeling, simulation, and performance evaluation analysis of a parabolic trough solar collector power plant coupled to an organic rankine cycle engine in north eastern greece using trnsys," *Journal of Solar Energy Engineering*, vol. 141, no. 6, p. 061004, 05 2019. [Online]. Available: https://doi.org/10.1115/1.4043658

[3] M. Petrollese, G. Cau, and D. Cocco, "The Ottana solar facility: dispatchable power from small-scale CSP plants based on ORC systems," *Renewable Energy*, vol. 147, pp. 2932–2943, 2020, oRC in Renewable Energy Systems, ORC 2017 Special Issue. [Online]. Available: https://doi.org/10.1016/j.renene.2018.07.013

[4] Y.-L. He, D.-H. Mei, W.-Q. Tao, W.-W. Yang, and H.-L. Liu, "Simulation of the parabolic trough solar energy generation system with organic rankine cycle," *Applied Energy*, vol. 97, pp. 630–641, 2012, energy Solutions for a Sustainable World - Proceedings of the Third International Conference on Applied Energy, May 16-18, 2011 - Perugia, Italy. [Online]. Available: https://doi.org/10.1016/j.apenergy.2012.02.047

[5] M. Borunda, O. Jaramillo, R. Dorantes, and A. Reyes, "Organic rankine cycle coupling with a parabolic trough solar power plant for cogeneration and industrial processes," *Renewable Energy*, vol. 86, pp. 651–663, 2016. [Online]. Available: https://doi.org/10.1016/j.renene.2015.08.041

[6] L. Tocci, T. Pal, I. Pesmazoglou, and B. Franchetti, "Small scale organic rankine cycle (ORC): A techno-economic review," *Energies (MDPI)*, vol. 10, no. 4, p. 413, 2017. [Online]. Available: https://doi.org/10.3390/en10040413

[7] H.-C. Jung and C. Y. Cha, "Sizing a parabolic trough collectoe for a micro solar organic rankine cycle," *Jurnalteknologi(Sciences Engineering)*, vol. 81, no. 2, p. 123 – 133, 2019. [Online]. Available: https://doi.org/10.11113/jt.v81.12304

[8] A. R. Archibold, J. Gonzalez-Aguilar, M. M. Rahman, D. Yogi Goswami, M. Romero, and E. K. Stefanakos, "The melting process of storage materials with relatively high phase change temperatures in partially filled spherical shells," *Applied Energy*, vol. 116, pp. 243–252, 2014. [Online]. Available: https://doi.org/10.1016/j.apenergy.2013.11.048

[9] G. Zhu, C. Turchi, D. Wendt, G. Mines, S. Cohan, L. Angelini, F. Bizzarri, D. Consoli, and A. Marzo, "Stillwater hybrid geo-solar power plant optimization analyses," pp. 891–900, 2015, publisher Copyright: © Copyright (2015) by Geothermal Resources Council All rights reserved.; 39th Geothermal Resources Council Annual Meeting - Geothermal: Always On, GRC 2015 ; Conference date: 20-09-2015 Through 23-09-2015. [Online]. Available: https://www.scopus.com/pages/publications/84964031577

[10] H. GunhanOzcan, H. Gunerhan, N. Yildirim, and A. Hepbasli, "A comprehensive evaluation of PV electricity production methods and life cycle energy-cost assessment of a particular system," *Journal of Cleaner Production*, vol. 238, no. 2, p. 117883, 2019. [Online]. Available: https://doi.org/10.1016/j.jclepro.2019.117883

[11] M. Petrollese and D. Cocco, "Optimal design of a hybrid CSP-PV plant for achieving the full dispatchability of solar energy power plants," *Solar Energy*, vol. 137, no. 2016, p. 477–489, 2016. [Online]. Available: https://doi.org/10.1016/j.solener.2016.08.027

[12] D. V., K. G., S. M., and K. D., "Test results segs ls-2 solar collector, New Mexico," *Sandia National Laboratories*, December 1994. [Online]. Available: https://doi.org/10.2172/70756

[13] J. Z. Alvi, Z. Guan, and M. Imran, "Thermoeconomic evaluation and sustainability insights of hybrid solar–biomass powered organic rankine cycle systems: A comprehensive review," *Biomass*, vol. 4, no. 4, pp. 1092–1121, 2024. [Online]. Available: https://doi.org/10.3390/biomass4040061

[14] H. Berrebah, T. Baki, and M. Tebbal, "Comprehensive investigation of solar water heater system performance, stratification, charging,

and discharging efficiency using TRNSYS software," *Acta Mechanica Slovaca*, vol. 28, no. 1, pp. 26–36, 2024. [Online]. Available: https://doi.org/10.21496/ams.2024.005

[15] M. Lazreg, T. Baki, and D. Nehari, "Influence of the number of tanks on the performance of a domestic solar water heater," *Acta Mechanica Slovaca*, vol. 27, no. 4, pp. 14–21, 2023. [Online]. Available: https://doi.org/10.21496/ams.2023.037

[16] S. A. Klein *et al.*, "Trnsys 16.1: A transient system simulation program," *Mathematical Reference*, 2007. [Online]. Available: http://sel.me.wisc.edu/trnsys

[17] A. Khelif, A. Talha, M. Belhamel, and A. H. Arab, "Feasibility study of hybrid diesel–PV power plants in the southern of Algeria: case study on Afra power plant." *International Journal of Electrical Power and Energy Systems*, vol. 43, no. 1, p. 546–553, 2012. [Online]. Available: https://doi.org/10.1016/j.ijepes.2012.06.053

[18] S. Quoilin, J. Lebrun, and V. Lemort, "Experimental study and modeling of an organic rankine cycle using scroll expander," *Journal of Applied Energy*, vol. 87, no. 4, pp. 1260–1268, 2010. [Online]. Available: https://doi.org/10.1016/j.apenergy.2009.06.026

[19] Duffie and Beckman, "Solar engineering of thermal processes," *John Wiley and Sons*, p. 122905, 2013. [Online]. Available: https://doi.org/10.1002/9781118671603

[20] S. K. Panja, B. Das, and V. Mahesh, "Performance evaluation of a novel parabolic trough solar collector with nanofluids and porous inserts," *Applied Thermal Engineering*, vol. 258, p. 124495, 2025. [Online]. Available: https://doi.org/10.1016/j.applthermaleng.2024.124495

[21] A. AlZahrani and I. Dincer, "Energy and exergy analyses of a parabolic trough solar power plant using carbon dioxide power cycle," *Energy Conversion and Management*, vol. 158, pp. 476–488, 2018. [Online]. Available: https://doi.org/10.1016/j.enconman.2017.12.071

[22] S. Quoilin, M. Orosz, H. Hemond, and V. Lemort, "Performance and design optimization of a low-cost organic rankine cycle for remote power generation," *Solar Energy*, vol. 85, pp. 955–966, January 2011. [Online]. Available: https://doi.org/10.1016/j.solener.2011.02.010

[23] T. Alqahtani, "Performance evaluation of a solar thermal storage system proposed for concentrated solar power plants," *Applied Thermal Engineering*, vol. 229, p. 120665, 2023. [Online]. Available: https://doi.org/10.1016/j.applthermaleng.2023.120665

[24] S. Baral, "Experimental and techno-economic analysis of solar-geothermal organic rankine cycle technology for power generation in nepal," *International Journal of Photoenergy*, vol. 2019, no. 1, p. 5814265, 2019. [Online]. Available: https://doi.org/10.1155/2019/5814265

[25] NREL, "System advisor model (SAM)," *National Renewable Energy Laboratory*, 2024. [Online]. Available: https://sam.nrel.gov/

[26] M. Villalva, J. Gazoli, and E. Filho, "Comprehensive approach to modeling and simulation of photovoltaic arrays," *IEEE Transactions on Power Electronics*, vol. 24, no. 5, pp. 1198–1208., 2009. [Online]. Available: http://dx.doi.org/10.1109/TPEL.2009.2013862

[27] V. Ramasamy, D. Feldman, J. Desai, and R. Margolis, "U.S. solar photovoltaic system and energy storage cost benchmarks," *National Renewable Energy Laboratory NREL* , 2021. [Online]. Available: https://www.nrel.gov/docs/fy22osti/80694.pdf

[28] D. Talavera, E. Muñoz-Cerón, J. Ferrer-Rodríguez, and P. J. Pérez-Higueras, "Assessment of cost-competitiveness and profitability of fixed and tracking photovoltaic systems: The case of five specific sites," *Renewable Energy*, vol. 134, pp. 902–913, 2019. [Online]. Available: https://doi.org/10.1016/j.renene.2018.11.091

[29] F. Mandys, M. Chitnis, and S. Silva, "Levelized cost estimates of solar photovoltaic electricity in the United Kingdom," *Patterns*, vol. 4, no. 5, p. 100735, 2023. [Online]. Available: https://doi.org/10.1016/j.patter.2023.100735

[30] R. Barbosa, B. Escobar, V. M. Sánchez, and J. Ortegón, "Effects of the size and cost reduction on a discounted payback period and levelized cost of energy of a zero-export photovoltaic system with green hydrogen storage," *Heliyon*, vol. 9, no. 6, p. e16707, 2023. [Online]. Available: https://doi.org/10.1016/j.heliyon.2023.e16707

[31] N. Ludin, N. Alyssa, K. Purvis-Roberts, A. Ahmad, M. Ibrahim, K. Sopian, and S. Jusoh, "Environmental impact and levelised cost of energy analysis of photovoltaic systems: in selected Asia pacific region: A cradle-to-grave approach," *Sustainability*, vol. 13, no. 1, p. 396, 2021. [Online]. Available: https://www.mdpi.com/2071-1050/13/1/396

[32] E. Ardeh, R. Loni, G. Najafi, B. Ghobadian, E. Bellos, and D.Wen, "Exergy and economic assessments of solar organic rankine cycle system with linear V-Shape cavity," *Energy Conversion and Management*, vol. 199, no. 5, p. 111997, 2019. [Online]. Available: https://doi.org/10.1016/j.enconman.2019.111997

[33] R. Vikas, V. Irappa, R. Shreyas, P. Garg, M. S., and N. Thirumalai, "Techno-economic comparison of solar organic rankine cycle (ORC) and photovoltaic (PV) systems with energy storage," *Renewable Energy*, vol. 113, no. 1, pp. 1250–1260, 2017. [Online]. Available: https://doi.org/10.1016/j.renene.2017.06.107

[34] S. Baral, D. Kim, E. Yun, and K. Kim, "Experimental and thermoeconomic analysis of small-scale solar organic rankine cycle (SORC) system," *Entropy*, vol. 17, no. 4, pp. 2039–2061, 2015. [Online]. Available: https://doi.org/10.3390/e17042039

[35] D. Young-Woo, B. Seung-Min, B. Seung-Yun, J. Hyeon-Ho, K. Yeon-Soo, K. Yong-Joo, and K. Wan-Soo, "Determining exhaust emissions (CO, NOx, PM) for a combine harvester based on measured engine load and emission factors using pems during actual field operation," *Computers and Electronics in Agriculture*, vol. 231, p. 110026, 2025. [Online]. Available: https://doi.org/10.1016/j.compag.2025.110026

How to cite this article:
A. Touil, D. Nehari, M. Laissaoui, and H. Benzaama. (2026). 'Thermodynamic analysis of small-scale CSP based on ORC systems compared with PV systems in North Africa zone. (Algeria as a case study)', Al-Qadisiyah Journal for Engineering Sciences, 19(1), pp. 098-109. https://doi.org/10.30772/qjes.2025.156874.1486